

# The extended narrow line region of NGC 4151

## I. Emission line ratios and their implications

M.V. Penston<sup>1</sup>, A. Robinson<sup>2</sup>, D. Alloin<sup>3</sup>, I. Appenzeller<sup>4</sup>, I. Aretxaga<sup>5</sup>, D.J. Axon<sup>6</sup>, T. Baribaud<sup>3</sup>, P. Barthel<sup>7</sup>, S.A. Baum<sup>8</sup>, C. Boisson<sup>3</sup>, A.G. de Bruyn<sup>8</sup>, J. Clavel<sup>9</sup>, L. Colina<sup>10</sup>, M. Dennefeld<sup>11</sup>, A. Díaz<sup>5</sup>, M. Dietrich<sup>12</sup>, F. Durret<sup>11</sup>, J.E. Dyson<sup>13</sup>, P. Gondhalekar<sup>14</sup>, E. van Groningen<sup>15</sup>, P. Jablonka<sup>3</sup>, N. Jackson<sup>6</sup>, W. Kollatschny<sup>12</sup>, E. Laurikainen<sup>16</sup>, A. Lawrence<sup>17</sup>, J. Masegosa<sup>18</sup>, I. McHardy<sup>19</sup>, E.J.A. Meurs<sup>20</sup>, G. Miley<sup>21</sup>, M. Moles<sup>18</sup>, P. O'Brien<sup>22</sup>, C. O'Dea<sup>8</sup>, A. del Olmo<sup>18</sup>, A. Pedlar<sup>6</sup>, J. Perea<sup>18</sup>, E. Pérez<sup>23</sup>, I. Pérez-Fournon<sup>23</sup>, J. Perry<sup>2</sup>, G. Pilbratt<sup>24</sup>, M. Rees<sup>2</sup>, I. Robson<sup>25</sup>, P. Rodríguez-Pascual<sup>9</sup>, J.M. Rodríguez Espinosa<sup>23</sup>, M. Santos-Lleo<sup>9</sup>, R. Schilizzi<sup>8</sup>, G. Stasińska<sup>3</sup>, G.M. Stirpe<sup>26</sup>, C. Tadhunter<sup>1</sup>, E. Terlevich<sup>27</sup>, R. Terlevich<sup>27</sup>, S. Unger<sup>1</sup>, V. Vila-Vilaró<sup>23</sup>, J. Vilchez<sup>23</sup>, S.J. Wagner<sup>4</sup>, M.J. Ward<sup>1</sup>, and G.J. Yates<sup>6</sup>

<sup>1</sup> Royal Greenwich Observatory, Madingley Road, Cambridge CB3 0EZ, United Kingdom

<sup>2</sup> Institute of Astronomy, Madingley Road, Cambridge CB3 0HA, United Kingdom

<sup>3</sup> Observatoire de Paris, Place Jules Janssen, F-92195 Meudon Principal Cedex, France

<sup>4</sup> Landessternwarte, Königstuhl, D-6900 Heidelberg, Federal Republic of Germany

<sup>5</sup> Depto. Física C-XI, Universidad Autónoma, Cantoblanco, E-28049 Madrid, Spain

<sup>6</sup> Nuffield Radio Astronomy Laboratory, Jodrell Bank, Macclesfield, Cheshire SK11 9DL, United Kingdom

<sup>7</sup> Kapteyn Astronomical Institute, P.O.Box 800, NL-9700 AV Groningen, The Netherlands

<sup>8</sup> Radiosterrewacht, Postbus 2, NL-7990 AA Dwingeloo, The Netherlands

<sup>9</sup> IUE Observatory, ESA, Apartado 54065, E-28080 Madrid, Spain

<sup>10</sup> ESA Astrophysics Division, Space Telescope Science Institute, Baltimore, MD21218, USA

<sup>11</sup> Institut d'Astrophysique, 98 bis, Blvd. Arago, F-75014 Paris, France

<sup>12</sup> Universitäts-Sternwarte, Geismarlandstraße 11, D-3400 Göttingen, Federal Republic of Germany

<sup>13</sup> Astronomy Department, University of Manchester, Manchester M13 9PL, United Kingdom

<sup>14</sup> Rutherford Appleton Laboratory, Chilton, Didcot, Berks OX1 0QX, United Kingdom

<sup>15</sup> Uppsala Astronomical Observatory, Box 515, S-75120 Uppsala, Sweden

<sup>16</sup> Turku Observatory, Tuorla, SF-21500 Pikkio, Finland

<sup>17</sup> Queen Mary College, University of London, Mile End Road, London E1, United Kingdom

<sup>18</sup> Instituto de Astrofísica de Andalucía, Apartado 2144, E-18080 Granada, Spain

<sup>19</sup> Department of Astrophysics, Nuclear Physics Laboratory, Keble Road, Oxford OX1 3RH, United Kingdom

<sup>20</sup> ESO, Karl-Schwarzschild-Straße 2, D-8046 Garching bei München, Federal Republic of Germany

<sup>21</sup> Sterrewacht Leiden, PO Box 9513, NL-2300 RA Leiden, The Netherlands

<sup>22</sup> Dept. of Astronomy, University College London, Gower Street, London WC1E 6BT, United Kingdom

<sup>23</sup> Instituto de Astrofísica de Canarias, E-38200 La Laguna, Tenerife, Spain

<sup>24</sup> ESA Astrophysics Division, ESTEC, Postbus 299, NL-2200 AG Noordwijk, The Netherlands

<sup>25</sup> School of Physics and Astronomy, Lancashire Polytechnic, Preston PR1 2TQ, United Kingdom

<sup>26</sup> Osservatorio Astronomico di Bologna, Via Zamboni 33, I-40126 Bologna, Italy

<sup>27</sup> Royal Greenwich Observatory, Herstmonceux Castle, Hailsham, East Sussex BN27 1RP, United Kingdom

Received September 25, 1989; accepted April 5, 1990

**Abstract.** This paper presents the first results from long-slit spectra of the Seyfert galaxy NGC4151 which give average diagnostic ratios of weak lines in the Extended Narrow Line Region (ENLR) of that galaxy and the first direct density measurement in an ENLR. These data confirm that the ENLR is kinematically undisturbed gas in the disc of the galaxy which is illuminated by an ionizing continuum stronger by a factor of 13 than a power law interpolated between recently observed ultraviolet and X-ray fluxes. Explanations of this apparent excess include a hot thermal continuum, time variations and an anisotropic radiation field.

We give reasons for favouring anisotropy which might be caused by shadowing by a thick accretion disc or by relativistic beaming. Shadowing by a molecular torus is unlikely, given the absence of an infrared signal from the reradiated flux absorbed by any torus. Anisotropy would have important implications for the bolometric luminosity and nature of active galactic nuclei.

**Key words:** Seyfert galaxies, Individual galaxies (NGC 4151), Emission line diagnosis, Interstellar medium: radiation field, Radiation mechanisms

Send offprint requests to: M.V. Penston

## 1. Introduction

Seyfert galaxies were classified by Khachikian & Weedman (1974) on the basis of the widths of their emission lines. Type 1 Seyferts have permitted lines with widths of order  $10\,000\text{ km s}^{-1}$ ; all lines of Type 2s (and forbidden lines of Type 1s) have widths in the range  $300 - 1\,000\text{ km s}^{-1}$ . The lines are emitted from gas in the Broad Line Region (BLR) and the Narrow Line Region (NLR) respectively; the different kinematic properties of each region accounting for the difference in line width. In both cases, the source of excitation of the gas is the hard ultraviolet continuum from the active nucleus.

More recently, a third region of high excitation line emission has been identified in an increasing number of active galaxies (Unger et al. 1987; Bergeron & Durret 1987). These regions are more extended spatially than the NLRs and have much smaller ( $\leq 30\text{ km s}^{-1}$ ) velocity dispersion (Unger et al. 1987). Unger et al. have called this the Extended Narrow Line Region or ENLR.

Studies of this region have led to the hypothesis that it is kinematically undisturbed gas in the disc of the active galaxy that is illuminated by a beam of ionizing ultraviolet light from the nucleus. Thus the morphology of the ENLR has been used to support the notion of Anisotropic Continuum Emission (see Ward 1988). Because the photoionization of this gas is easier to model than that of the NLR, where shocks driven by the radio-emitting plasma are thought to play a rôle (Pedlar, Dyson & Unger 1985; Wilson & Ulvestad 1987) the ENLR is the preferred site for a theoretical study of the spectrum of the ionizing source in the region at and beyond the Lyman limit.

Much excitement also surrounds the possibly related highly excited emission regions around radio galaxies<sup>1</sup> (for the particularly striking example of Pks2152-69, see di Serego Alighieri et al. 1988 and references therein). This subject was much discussed at the ESO workshop on Extranuclear Activity in Galaxies in May 1989 (see in particular Fosbury (1989) and references therein) and the existing state of knowledge is further reviewed by Tadhunter (1989).

In the particular galaxy we are discussing in this paper, the famous type 1 Seyfert galaxy NGC4151, the presence of the ENLR can be seen in the data of Ulrich (1973) who called it Cloud III. In more recent data, the spatial distribution of the ENLR can be seen on narrow band images (Heckman & Balick 1983; Pérez et al. 1989; Pérez-Fournon & Wilson 1989) and, in particular, on imaging Fabry-Perot TAURUS data (Unger et al. 1989), where the ENLR can be separated kinematically from the brighter more compact NLR. It contains several bright knots forming an elongated structure oriented at a position angle of  $\sim 50^\circ$  with the south-west side brighter (see Fig. 1). This position angle is close to that of the VLBI source in the nucleus of the galaxy (Harrison et al. 1986) but appears more misaligned with the larger radio structure and optical nuclear polarization

<sup>1</sup> The nomenclature ENLR has also been used to cover these extragalactic extended regions. There may however be good reason to review this usage before confusion arises. It may be that photoionization by an anisotropic source operates in both cases. However it would be wise to distinguish cases where the sharpness of the emission lines indicates a low velocity dispersion (e.g. undisturbed galactic rotation) low enough to exclude shock ionization being an important effect. In this work the phrase, ENLR, will be reserved for the very sharp line emitting region alone.

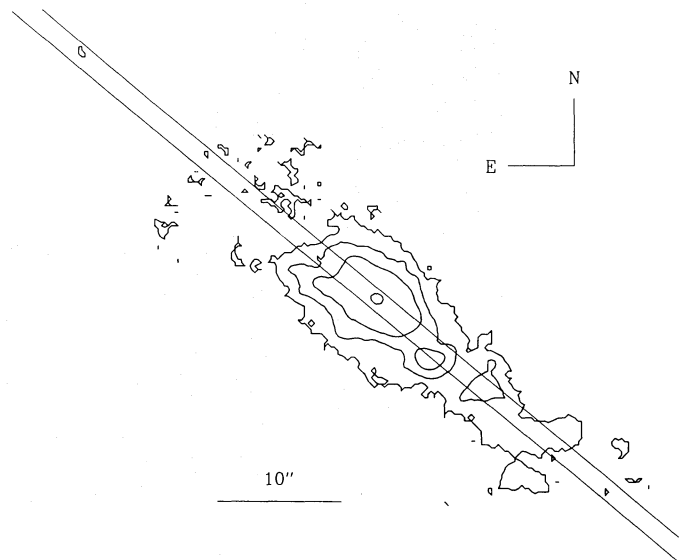


Fig. 1. A sketch map of the ENLR showing the slit orientation. The innermost contour marks the nucleus. (after Pérez et al. 1989)

(Schmidt & Miller 1980). We note, however, that the extended narrow line regions discovered in other galaxies display a wide variety of sizes and morphologies and, for this reason, the ENLR of NGC4151 should not necessarily be regarded as a prototype.

Data on the ultraviolet CIV and CIII lines from the ENLR of NGC4151 have been obtained by Bruhweiler & Smith (1988) who deduce the ionization parameter in this region. A second study of the physical conditions in the ENLR using optical spectrophotometry has been undertaken by Schulz (1988) who gives ratios for a few of the stronger optical lines in NGC4151.

In this paper, we extend his work using new spectra to both increase the wavelength coverage and measure the line ratios of fainter lines. We expect to analyse our spectra in fuller detail in conjunction with further data in future papers. These will deal with the line surface brightness distribution of the emission along the slit and analyse the data on the kinematics of the ENLR and the stellar absorption lines.

## 2. Observations and Data Reduction

We obtained long-slit spectra of NGC4151 using the 235 mm camera of the Intermediate Dispersion Spectrograph and the Image Photon Counting System on the Isaac Newton Telescope at the *Observatorio del Roque de los Muchachos* on La Palma. Each spectrum contains  $2040 \times 120$  pixels of  $0.52\text{ \AA}$  in the spectral direction and  $1.47\text{ arcsec}^2$  in the spatial direction respectively. This implies a spectral resolution of about  $1\text{ \AA}$  or  $60\text{ km s}^{-1}$ . During 1989 May 5/6th we obtained three spectra covering the wavelength ranges  $\lambda\lambda 3150-4200, 4100-5150$  and  $5900 - 6950$  each with a  $1.5\text{ arcsec}$  slit oriented along the

<sup>2</sup> At the distance of NGC4151, assuming a Hubble constant of  $50\text{ km s}^{-1}\text{ Mpc}^{-1}$ ,  $1\text{ arcsec}$  corresponds to  $97\text{ pc}$ .

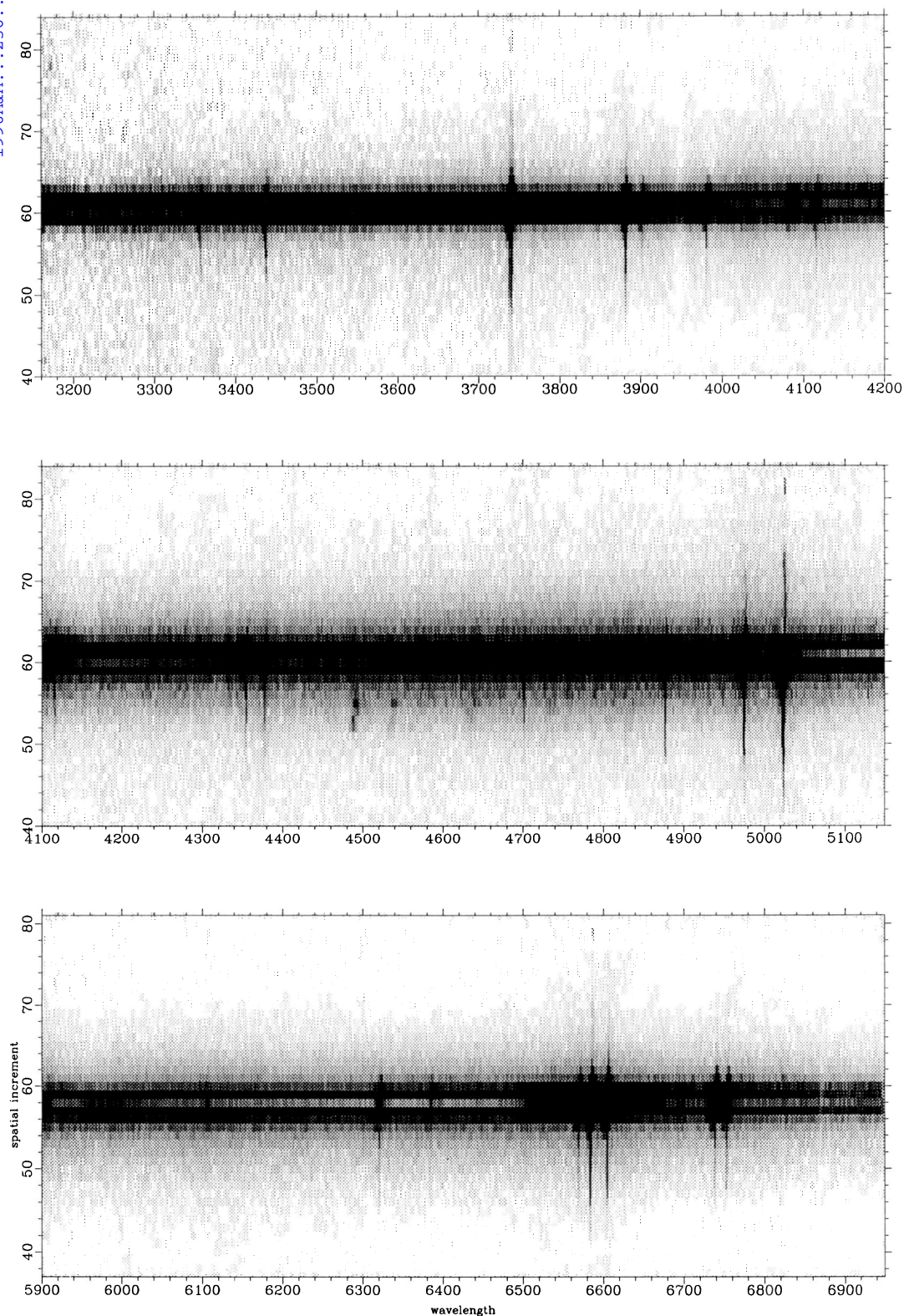


**Fig. 2.** A grey scale representation of our three long-slit spectra of NGC4151 taken at position angle  $51^\circ$ . The wavelengths increase from left to right; the north-west region lies above and the south-west below the spectra. The sharp lines extending over many 1.5 arcsec pixels from the nucleus come from the ENLR. The nuclear continuum, BLR and NLR are partially hidden behind an occulting 'finger'. The slight curvature of the spectra is caused by atmospheric dispersion. The top spectrum covers 3150 - 4200 Å and shows the lines of [NeV] (twice), [OII] (note the resolution of the doublet), [NeIII], HeI, [NeIII], [SII] and  $H\delta$ . The middle spectrum covers 4100 - 5150 Å and shows  $H\delta$  (just at the edge),  $H\gamma$ , [OIII], HeII,  $H\beta$  and the two nebular lines of [OIII]. Note the optical 'ghost' images of [OIII] and  $H\beta$  near  $\lambda 4500$ . The bottom spectrum covers 5900 - 6950 Å and shows [FeVII] (faintly), [OI] (twice), [NII],  $H\alpha$ , [NII] and the [SII] doublet.

**Table 1.** Emission line ratios in the ENLR of NGC4151 Observed and corrected for a reddening of  $E_{B-V} = 0.05$  ( $H\beta = 100$ )

Species	$\lambda_0$	Ratio		Species	$\lambda_0$	Ratio	
		Obs	Corr			Obs	Corr
[NeV]	3346	21	22	HeII	4686	38	38
[NeV]	3426	60	64	H $\beta$	4861	100	100
[OII]	3726	108	112	[OIII]	4959	435	434
[OII]	3729	136	138	[OI]	6300	25	23
[NeIII]	3869	100	104	[OI]	6364	7	7
H $\zeta$ /HeI	3889	12	12	[NII]	6548	40	38
[NeIII] H $\epsilon$	3968	61	63	H $\alpha$	6563	280	265
[SII]	4072	10	10	[NII]	6584	122	116
H $\delta$	4102	16	17	[SII]	6717	56	53
H $\gamma$	4340	42	43	[SII]	6731	48	46
[OIII]	4363	24	24				

ENLR at position angle  $51^\circ$ . The exposure times were 4 300, 3 700 and 7 200 s respectively giving approximately equal sensitivity in each wavelength range. For the observations under discussion here, differential refraction perpendicular to the slit is never more than 0.5 arcsec.

For our observations, the nucleus of NGC4151 was placed behind an occulting ‘finger’ to cut down the light from the nucleus, BLR and NLR and to minimize saturation problems. Even so the [OIII]  $\lambda 5007$  line in the remaining NLR was saturated and beam-pulling effects in the IPCS may affect data on this line in the ENLR so that it was not used in the following. An optical ‘ghost’ is present in the spectrograph and causes spurious images of the H $\beta$  and the nebular lines of [OIII] from the NLR to appear at wavelengths near  $\lambda 4500$  below (i.e. south-west of) the nucleus. Fortunately these do not affect important ENLR lines.

Calibration exposures of standard stars for each wavelength range and a later low dispersion ( $2.08 \text{ \AA}$  per pixel) spectrum of NGC4151 (to tie together the different spectral regions) were also obtained.

The data were reduced in the standard way using the FIGARO software (Fuller 1989) on the La Palma Data Reduction VAX 8300. The spectra are illustrated in Fig. 2 after wavelength and flux calibration and sky-subtraction but with no ‘slit-flattening’ performed. The long-slit spectra show emission beyond that visible on narrow-band imaging data and the data of Unger et al. (1989).

Here we give only ratios of emission lines integrated over the brightest part of the ENLR, the region within the slit lying between 6 and 20 arcsec to the south-west of the nucleus, anticipating a fuller more detailed discussion in later papers. These ratios are adequate to investigate the ionization mechanism of and the physical conditions in the ENLR. The only previous work on optical ENLR line ratios in NGC4151 (Schulz 1988) was restricted to strong lines longward of H $\beta$  within 12 arcsec of the nucleus. We are sensitive to lines as faint as about 5% of H $\beta$ .

A plot of the sky-subtracted spectrum from this region is shown in Fig. 3 and line ratios are given in Table 1 normalized to  $H\beta = 100$  and corrected for a reddening of  $E_{B-V} = 0.05$  (Penston et al. 1981). We adopt an overall error estimate of 5% of H $\beta$  or 0.1 times the ratio (whichever is greater) for the line ratios in the Table where the lines being ratioed are well

separated in wavelength. This prescription is in accord with our measurements of the known fixed ratios of [NeV], [NeIII], [OI], [NII] and the Case B Balmer series ratios. However the errors on the doublet ratios do not involve the flux calibration and are therefore smaller. These were investigated using both line fitting and pure photon counting algorithms. In the case of [SII] where the lines are unblended statistical errors provide the major source of uncertainty; for [OII], line blending (primarily separating the broader NLR line) dominates. The deduced errors are given for the doublet ratios in the next section and, with the prescription for widely separated lines, are used for propagating the errors through the calculations in the next sections.

The line ratios in Table 1 generally resemble those of the NLRs in Seyfert 1.5s and 2s (e.g. Koski 1978; Cohen 1983) and of other ENLRs (e.g. Unger et al. 1987 for [OIII] H $\beta$ ; Robinson et al. 1987; Pogge 1989) although they have a somewhat higher excitation level than those in the NLR of NGC4151 itself (see also Bergeron et al. (1983).

### 3. Physical Conditions in the ENLR

#### 3.1. Diagnosis of Density and Temperature

The relative intensities of the lines in Table 1 include four line ratios useful for an immediate diagnosis of the electron density,  $n_e$ , and temperature,  $T_e$ , of the emitting gas in the ENLR. These are the [OII] and [SII] doublet ratios  $\lambda 3726/\lambda 3729$  and  $\lambda 6717/\lambda 6731$  which are sensitive to the density and the [OIII] auroral to nebular line ratio  $\lambda 4363/\lambda 4959$  and the [SII] blue-to-red ratio  $\lambda 4072/6724$  which are sensitive to the temperature at low densities. We find:

$$\begin{aligned}
 I_{3729}/I_{3726} &= 1.24 \pm 0.12 & : \text{[OII]} \\
 I_{6717}/I_{6731} &= 1.14 \pm 0.10 & : \text{[SII]} \\
 I_{4363}/3 \times I_{4959} &= 0.018 \pm 0.004 & : \text{[OIII]} \\
 I_{4072}/(I_{6717} + I_{6731}) &= 0.10 \pm 0.05 & : \text{[SII]}
 \end{aligned}$$

corresponding to values of  $\log n_e = 2.25 \pm 0.21$  and  $2.40 \pm 0.17$  from [OII] and [SII] doublet ratios respectively and  $\log T_e = 4.15 \pm 0.03$  and  $4.3 \pm 0.3$  from [OIII] and [SII] blue-to-red respectively (Aller 1987). Note that the [OII] and [SII] doublet

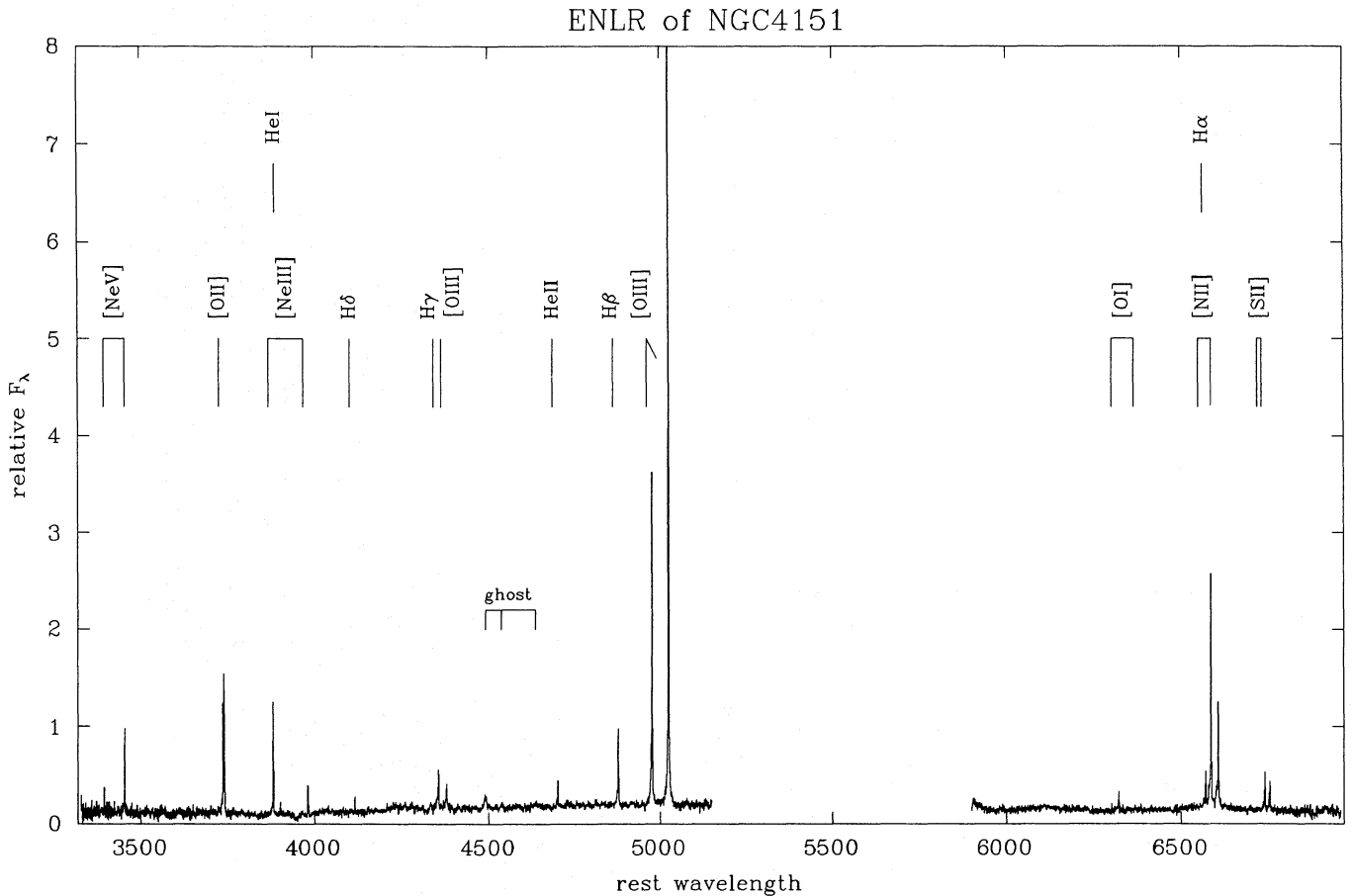


**Fig. 3.** The relative flux from the ENLR of NGC4151 plotted against wavelength. This spectrum is the sum of the emission within a 1.5 arcsec slit at position angle  $51^\circ$  between 6 and 20 arcsec from the nucleus. The lines are very sharp and faint features such as HeI  $\lambda 3889$  and [OI]  $\lambda 6364$  are discernible. Note that the broad features near 4500 Å are spurious; a result of the optical 'ghosts' of H $\beta$  and the nebular lines of [OIII].

ratios are respectively more than 2 and more than  $3\sigma$  from their low density limits. Our overall value of  $\log n_e$  is  $2.34 \pm 0.13$  and of  $\log T_e$  is  $4.15 \pm 0.03$ . We note that the Schulz (1988) values of the [SII] doublet ratio are 1.1–1.3 in agreement with our value (as indeed are his other line ratios).

The single-point approximation used in such a diagnosis is oversimplified. Obviously the ENLR will contain material with a range of densities and temperatures (cloud and intercloud regions in the interstellar medium of the galaxy). This is accentuated by averaging over the slit although such problems will not be entirely eliminated by spatial resolution. The resulting densities and temperatures should be broadly interpreted as average emissivity-weighted estimates.

Turning to the high excitation lines, a notable feature of Table 1 is the strength of [NeV] and HeII. The HeII line can only be present at such a strength if the emitting gas is photoionized by a hard ultraviolet continuum or ionized by high velocity (over  $100 \text{ km s}^{-1}$ ) shocks (Binette, Dopita & Tuohy 1985). However in the case of the ENLR, we can rule out shocks because the velocity dispersion of the gas is  $\leq 30 \text{ km s}^{-1}$  (Unger et al. 1987) much less than the required shock velocities. In addition the low temperature derived above is incompatible with the ionization being dominated by shocks while it agrees with the predictions of the photoionized models described below. We conclude that the ionizing source is a hard ultraviolet continuum.

Concerning the nature of the ENLR, in addition to the previous kinematic evidence, we now find the electron density to be  $220 \pm 80 \text{ cm}^{-3}$ . This would be a high value for the mean density in a galactic disc but we must recall that it is an emissivity-weighted estimate. The densest clouds will be represented most strongly in the average. There will also be a dependence on covering factor: the larger clouds may also be denser.

These comparatively high values may imply that the ENLR lies close to the gaseous plane of NGC4151 where high density clouds will be more common. The close agreement between the ENLR and 21cm velocities (Unger et al. 1989) also supports this picture. A theoretical mechanism which could result in the collimation axis being oriented close to the plane has been discussed by Tohline & Osterbrock (1982). We note however the selection effects favouring the discovery of collimation axes in directions where gaseous material exists.

We warn that ENLR densities in NGC4151 may be higher than in other galaxies because the relatively small scale of the region, compared to that in some other galaxies, means that in this case the ENLR lies within the disc of NGC4151.

Our results are consistent with the pre-existing picture that the ENLR is undisturbed disc gas illuminated and ionized by the central source at the nucleus of the galaxy.

### 3.2. The ionization parameter in the ENLR

In order to go further in understanding of the ionization of the ENLR, comparison with photoionization models is required. One can then obtain an estimate of the ionization parameter, the ratio of the densities of ionizing photons and electrons in the emitting region. For isotropically emitting sources,  $U = Q/4\pi r^2 cn_e$ , where  $Q$  is the total number of ionizing photons emitted per unit time by the ionizing source and  $r$  is its distance from the ionized gas.

We postpone detailed modelling of the emission line spectrum until a later paper. Here we simply wish to determine the ionization parameter empirically from the measured relative intensities. We require a diagnostic which is sensitive to the ionization parameter but which is also reasonably insensitive to the other parameters which affect the relative emission line intensities, such as the ionizing continuum energy distribution, the density and the chemical abundances. The ratio of singly to doubly ionized oxygen  $\lambda 3727/\lambda 5007$  comes closest to meeting these criteria. We find:

$$(I_{3726} + I_{3729})/3 \times I_{4959} = 0.19 \pm 0.03$$

Fig. 4 shows the relationship between  $I_{3727}/I_{5007}$  and  $\log U$  for several sequences of photoionization models employing a variety of possible ionizing continua. The range of continua covers most of the possibilities which might be appropriate to active galactic nuclei and includes both hot blackbodies, ranging in temperature from  $10^5$  to  $210^5$  K, and power-laws with spectral indices,  $\alpha$ , between  $-2$  and  $-1$ . The models are taken from Robinson et al. (1987) and are all ionization bounded, with a constant gas density of  $100 \text{ cm}^{-3}$  and solar abundances (as listed in Binette, Courvoisier & Robinson 1988). Whereas  $I_{3727}/I_{5007}$  is sensitive to  $U$  over a wide range of values, it is relatively insensitive to the choice of continuum energy distribution. As the true shape of the EUV continuum is uncertain, this is an important property which makes this ratio more reliable as a diagnostic than other possible choices such as  $[\text{OII}]/\text{H}\beta$ . To an excellent approximation, the ionization parameter is inversely proportional to  $I_{3727}/I_{5007}$ , irrespective of the ionizing continuum. A least squares fit including all the points shown in Fig. 4 yields:

$$\log U = -2.74 - 1.00 \log I_{3727}/I_{5007}$$

with an rms residual in  $\log U$  of 0.2. For the measured value of  $I(3727/5007)$ , this expression yields  $\log U = -2.0 \pm 0.2$  where the error in  $U$  takes into account not only the error in the line ratio but also the residuals from the relationship shown in Fig. 4 and therefore assumes that the spectrum of the ionizing continuum is spanned by the various power law and thermal forms used for that figure.

The  $[\text{OII}]/[\text{OIII}]$  ratio is also sensitive, to differing degrees, to the other parameters which govern relative line intensities in photoionization models<sup>3</sup>. The average density which we have determined for the ENLR lies in the region where the  $[\text{OII}]$  lines begin to be collisionally suppressed. Nevertheless, the variation of  $I_{3727}/I_{5007}$  with  $n_e$  is still relatively slow and the range in  $I_{3727}/I_{5007}$  which corresponds to the error in our density

<sup>3</sup> The uncertainty introduced by the inherent differences between existing photoionization codes is small. Several of these codes were compared for a number of test cases in Péquignot (1986). In the case which approaches closest to the range of physical conditions of interest here, the rms deviation in  $I_{3727}/I_{5007}$  corresponds to  $\pm 0.1$  in  $\log U$ .

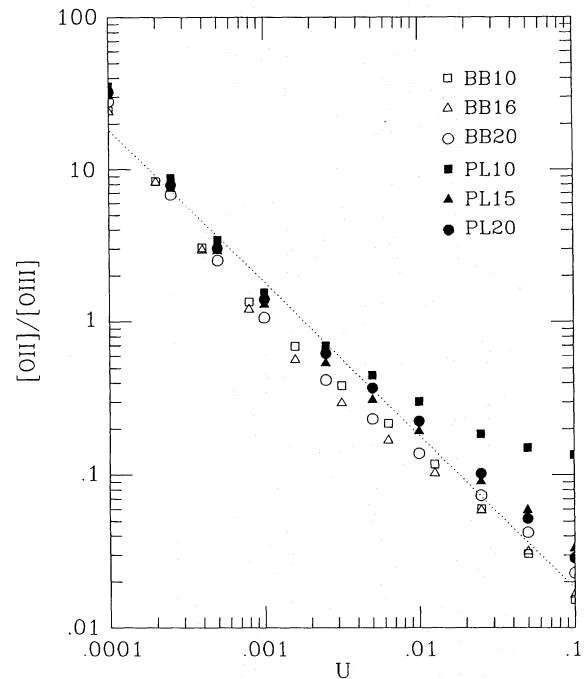


**Fig. 4.** The relationship between the intensity ratio  $[\text{OII}]\lambda 3727/[\text{OIII}]\lambda 5007$  and the ionization parameter,  $U$ , for several series of photoionization models employing both power-law and blackbody ionizing continua. Each series is identified by a code whose last two digits indicate either the blackbody temperature in units of 10,000 K or the power-law spectral index (1.0, 1.5 or 2.0). The models are taken from Robinson et al. (1987). All are ionization bounded, have a constant gas density of  $100 \text{ cm}^{-3}$  and solar abundances. A least squares fit to the combined set of models (dotted line) gives  $\log U = -2.74 - 1.00 \log I_{3727}/I_{5007}$  with an rms residual in  $\log U$  of 0.2.

measurement only introduces a small uncertainty of about 0.1 in  $\log U$ .

The element abundances, which can only be determined by detailed modelling of the entire emission line spectrum, are a potentially more serious source of uncertainty. This will have increased the derived  $\log U$  by  $+0.2$  if the ENLR abundances are as low as 10% of the solar composition and decreased it by  $-0.5$  if, on the other hand, abundances are enhanced by a factor two. In what follows, we will assume that the ENLR has solar element abundances.

Ionization-bounded models which have an ionization parameter similar to the value derived above and which employ power-law ionizing continua similar to that adopted in Section 4.1 (i.e.  $\alpha \approx -1.5$ ) predict values of the  $[\text{OIII}]/\text{H}\beta$  ratio and indeed, relative intensities of the  $[\text{OII}]$ ,  $[\text{NII}]$ ,  $[\text{SII}]$  and  $[\text{OI}]$  lines, which are in reasonably good agreement with the observed spectrum. These models fail, however, to reproduce the observed strengths of the  $[\text{NeV}]$  and  $\text{HeII}$  lines relative to  $\text{H}\beta$  by factors of 2 or 3. This may suggest that a somewhat different continuum energy distribution, perhaps including a thermal component (see Section 4.2), is required. Alternatively, the strengths of these lines may indicate that the ENLR contains a substantial matter-bounded component. The presence of significant  $[\text{OI}]$  and  $[\text{SII}]$  emission demonstrates that optically thin gas does not dominate the line fluxes. It seems likely, nevertheless, that the ENLR contains a mixture of matter and radiation bounded clouds and this may affect our derivation of the ionization parameter. To

check the magnitude of the effect, we have examined linear combinations of optically thick and optically thin models taken from Stasińska (1982). Solving for the observed [NeV] strength yields a somewhat smaller value of  $I_{3727}/I_{5007}$  for the optically thick component than would be obtained from a purely optically thick model, and this in turn would cause us to overestimate  $\log U$  by up to +0.24. The effect is greatly reduced if the matter-bounded component has a higher ionization parameter (lower density) than the radiation-bounded component.

Our value of  $\log U$  is close to that deduced from the ultraviolet lines by Bruhweiler & Smith (1988),  $\log U = -1.7$ . These authors, however, associated a high density with the emitting material, noted that  $U$  should not then be greater than that applicable to the NLR and felt this to be a ‘problem’. With the low ENLR density that we find however, this difficulty is largely alleviated.

### 3.3. Flux of photons seen by ENLR

The morphology of the ENLR results from the combined spatial distribution of matter and radiation. We have shown that the source of ionization is hard ultraviolet radiation and estimated its ionization parameter. If this source is in the nucleus, either it is anisotropic so that it does not illuminate the whole surrounding region or the ENLR marks the presence of excess gas.

To investigate this, we now calculate the flux of ionizing photons seen by the ENLR gas with a view to comparing it with that emitted towards Earth.

We introduce a new parameter  $q = Ur^2cn_e$ , the flux of photons per unit solid angle. In a source emitting isotropically the total emitted flux of photons  $Q = 4\pi q$ . When anisotropy may be present  $q$  seems a more appropriate variable.

We use the values of  $\log n_e$  and  $\log U$  computed above. To calculate  $r$  we use 8.8 arcsec, the intensity-weighted mean angular distance from the nucleus to the ENLR whose light is in fact dominated by condensations at 6 and 13 arcsec from the nucleus. To calculate the projection angle between the ENLR and the plane of the sky, we adopted the inclination and position angle of the gaseous disc of NGC4151 (assuming, as discussed earlier, that the ENLR is directed quite close to the plane of that disc) both given by Davies (1973) as 26 degrees. For an ENLR position angle of 51 degrees, we find the projection angle is 12 degrees so that  $r = 8.8 \times 97 \sec 12^\circ = 870$  pc.

A little arithmetic then yields  $\log q_\perp = 53.7 \pm 0.3$  where  $q_\perp$  is the flux of ionizing photons per unit solid angle seen by the ENLR and the error follows from quadratically combining the errors in  $U$  and  $n_e$ , with some allowance for errors in  $r$ .

## 4. Comparison with Direct Observations from Earth

### 4.1. Comparison with a Power Law

The ionizing flux emitted in the direction of Earth is in fact impossible to observe and is difficult to determine with any certainty since these photons will suffer photoelectric absorption *en route* to Earth in the interstellar media of both NGC4151 and

the Milky Way. Moreover NGC4151 is variable and we need to compare with the ENLR which is responding to the light it has seen from the nucleus over the last few thousand years!

IUE observations of NGC4151 by Penston et al. (1981) offer us the best source of information. They studied NGC4151 during its high phase (unlike the period since 1981 when the galaxy has been fainter than in any decade in which the light curve exists, i.e. since 1915) and find the flux per unit wavelength interval at about 1200 Å to vary between 1 and  $3.5 \times 10^{-13}$  ergs cm<sup>-2</sup> s<sup>-1</sup> Å<sup>-1</sup>. They also find  $E_{B-V} = 0.05 \pm 0.05$ . Finally interpolation in their Fig.5 between the Lyman limit and the X-ray window suggests  $F_\nu \propto \nu^{-1.4}$  in this region.

Adopting  $F_\lambda(912 \text{ Å}) = 4 \times 10^{-13}$  ergs cm<sup>-2</sup> s<sup>-1</sup> Å<sup>-1</sup>

and an absorption at the Lyman limit  $A_{912} = 20 E_{B-V} = 1 \pm 1 \text{ mag}$ , we find the flux at Earth per unit frequency interval after correction for interstellar absorption:

$$F_{\nu_0} = 1.1 \times 10^{-25} \text{ ergs cm}^{-2} \text{ s}^{-1} \text{ Hz}^{-1},$$

give or take a factor of 2.5, and where  $\nu_0$  is the frequency of the Lyman limit,  $3.3 \times 10^{15}$  Hz.

Now using the formula for the number of ionizing photons per unit solid angle emitted in our direction in a power law spectrum:

$$q_\parallel = D^2 F_{\nu_0} / \alpha h$$

where  $h$  is Planck’s constant,  $D$  is the distance of NGC4151 and  $\alpha$  is the spectral index ( $F_\nu \propto \nu^{-\alpha}$ ), we find that, for the direction towards Earth,  $\log q_\parallel = 52.6 \pm 0.4$ . The error is dominated by the uncertainty in the extinction.

The two values of  $\log q$  differ<sup>4</sup> by  $1.1 \pm 0.5$  where the independent errors in the two estimates of  $q$  are combined quadratically. This corresponds to a factor of 13 (give or take a factor of 3) or, alternatively,  $2.8 \pm 1.2$  magnitudes. Although the errors are unlikely to be gaussian, these formal errors include all identified sources of systematic error (in addition to those of the line ratios). It is most likely that the difference is real. The major source of error is that in the extinction along the line of sight to NGC4151 (0.4 in  $\log q$ ). The error introduced by the photoionization modelling is half this.

We have shown that an observer in the ENLR of NGC4151 sees 13 times as many photons as would be expected from an isotropic power law source interpolated between recent ultraviolet and X-ray observations at Earth (or extrapolated from the recently observed optical/ultraviolet continuum).

### 4.2. Thermal Ionizing spectrum

The spectral shape of the ionizing spectrum considered in the last section was that of a power law. It is apparent that adopting instead a hot thermal spectrum would increase  $q_\parallel$ , because there are more photons in a harder spectrum fixed to an observed value near the Lyman limit. The presence of such a component, dominating the EUV continuum, would therefore decrease the discrepancy between  $q_\parallel$  and  $q_\perp$ .

Although we have no direct information on the shape of the ionizing continuum, constraints on the temperature and strength of a possible thermal component are imposed by the HeII/Hβ ratio in the ENLR and the slope of the continuum as seen in IUE data. As an example, we consider the combination of a hot blackbody superposed on an underlying power-law

<sup>4</sup> Note that the adopted value of the Hubble constant cancels out of this comparison.

which has a slope similar to the one we have assumed. The maximum temperature of a blackbody component which could dominate the ionizing photon flux is limited by the observed HeII/H $\beta$  ratio of 0.38 to around 160,000 K<sup>5</sup> (see Fig. 2b of Binette et al. 1988). If a strong blackbody-like component of this temperature is present, we would expect it to influence the slope of the continuum at wavelengths above the Lyman limit. In fact, IUE observations reveal an upturn in the ultraviolet continuum shortwards of 2000 Å (Penston et al. 1981; Perola et al. 1982). The strength of this upturn is highly variable and its nature under dispute but it is plausible that it is at least partly due to a (possibly thermal) component peaking in the EUV. Ascribing 50% of the 1455 Å continuum to the presence of a 160,000 K blackbody, corresponds to a situation in which the blackbody produces nearly 20 times the ionizing photon flux of an underlying power-law.

Evidently, both the HeII/H $\beta$  ratio and the ultraviolet continuum shape are consistent with the presence of a thermal component of sufficient strength to account for the entire discrepancy between  $q_{\parallel}$  and  $q_{\perp}$ . This emphasises that the uncertainties in the comparison of the values of  $q$  lie predominantly in the determination of  $q_{\parallel}$ .

However the linear geometry of the ENLR is not explained with an isotropically emitting thermal source. Because of this, we continue now to discuss further possible alternative explanations of the difference between  $q_{\parallel}$  and  $q_{\perp}$ . We shall return to the question of whether ionizing continua dominated by thermal components can reproduce the ENLR line ratios in a future paper.

## 5. Discussion

We note that a similar ‘photon deficit’ problem has been found in several other AGN using arguments based on the recombination line luminosities (Tadhunter 1989). There seem to be three ways to account for this difference. These are:

- a) local ionization within the ENLR,
- b) a time-delay explanation and
- c) anisotropic continuum emission.

We now discuss each in turn.

### 5.1. Local Ionization within the ENLR

The extended X-ray emission detected by Elvis, Briel & Henry (1983) is one possible source but such thermal X-rays do not ionize efficiently (Johnstone & Fabian 1988) and would in any case produce a LINER-type spectrum (e.g. Binette et al. 1985). A second possibility, ionization by very hot stars (either post-AGB stars or ‘warmers’), found only in the ENLR, seems contrived.

### 5.2. Time-delay Effects

Since it is 1-2 kiloparsecs in length, the ENLR we see is responding to light emitted by the nucleus of order 1,000 years before that reaching us directly. Thus one possible explanation

<sup>5</sup> Very high temperature blackbodies ( $T \sim 10^6$  K) also satisfy this constraint but are inconsistent with other line ratios.

of the difference in the estimates of  $q$  is that NGC4151, known to be a variable object, was brighter for the previous thousand years than it has been in this century. There is no way to test this directly because no photometric data exist prior to 1915. Nor does the idea that the nucleus was that much brighter in the past violate any information we have on AGN variability; indeed it is entirely possible.

However this potentially attractive explanation does not give a reason why the ENLR is anisotropic about the nucleus and confined to a linear structure. This idea would also predict that some ENLRs in other galaxies would indicate a fainter nuclear brightness than that expected from direct observation. A test awaits studies of the type we have conducted here for other AGN.

### 5.3. Anisotropic Radiation Field

In this picture the difference of a factor 13 in  $q$  is attributed to the fact that the nuclear source shines more brightly in the direction of the ENLR than it does towards us. This is consistent with the picture discussed in the introduction to this paper and is our favoured interpretation.

There are three possible causes for this anisotropy. One idea attributes the effect to anisotropic emission from a disc (Netzer 1985, 1987); the second is relativistic beaming (Orr & Browne 1982); the last invokes an isotropic ultraviolet source absorbed anisotropically, perhaps by a nuclear disc (Antonucci & Miller 1985; Chelli et al. 1987; Ward 1988; Barthel 1989). We feel the first is not an adequate explanation in this case as it is hard to see how the emission from a disc can be as anisotropic and as narrowly beamed as that we find here.

#### 5.3.1. Relativistic Beaming

This idea seems to explain a number of observational facts about radio sources (Antonucci 1988; Browne 1989) and may also apply to Seyfert galaxies like NGC4151. However these galaxies are not strong radio sources and are not observed to show bulk relativistic motion (although we caution that the radio weakness could simply mean the beams were pointing away from us and would itself make relativistic motion hard to detect). It is important to realise that a factor of 13 anisotropy is much smaller than that postulated in the beamed component of quasars. With the particular geometry we have adopted for the ENLR in NGC4151, a Lorentz  $\gamma$  factor of only 1.3 is required, compared with about 5 (Orr & Browne 1982) in radio galaxies and quasars.

A further argument against the beaming hypothesis is provided by the restricted range of line equivalent widths observed in Seyferts. If one is to reconcile this with the beaming hypothesis one must postulate that observed Seyferts have been selected to have a restricted range of orientation to the observer: either so that their beaming axes make large angles to the line of sight or so that the angle between the axis and the line of sight is uniformly small. Neither of these ideas seems easy to defend.

#### 5.3.2. Shadowing by a Disc

There is now considerable evidence for shadowing by discs in Seyfert galaxies. In several cases the ENLR is conical with quite



sharp edges (Pogge 1988; Tsvetsanov et al. 1989; Pérez-Fournon & Wilson 1989).

However the problems posed by the good correlations (e.g. Ward et al. 1988) between optical, infrared and X-ray continuum and BLR line intensities, covering a wide range of intrinsic luminosities in Active Galaxies generally, are difficult to account for in the shadowing picture. The components at these various wavelengths vary on typically different time-scales and are thus thought to be emitted from regions of different sizes. Thus it is not easy to imagine how they can all be shadowed in the same proportion at different wavelengths. The X-rays show much more rapid variations than any other component (Done et al. 1989) and pose the greatest problems in this connection. The simplest explanation would be that the anisotropy factor rarely exceeds the factor of order ten which is the typical width of the correlations.

There are two different scales on which shadowing discs have been considered. The first is the ‘molecular torus’; the second is the ‘thick accretion disc’.

#### *Molecular Torus.*

Evidence exists for dense, obscuring, molecular clouds in the nuclei (Kawara, Nishida & Gregory 1989 and references therein). It is very natural to extend this idea to the case of NGC4151 in view of the results here.

In NGC4151 the ENLR only subtends 1–2 % of the sky as seen from the nucleus (Schulz 1988). If the flux is initially emitted isotropically and reradiated in the far-infrared by (say) a dusty torus, the total luminosity would be about 13 times greater than has previously been supposed. This reradiation should however be observable, for example, by the IRAS satellite. Integrating the observed infrared continuum given by Edelson et al. (1988) between 2 and 100  $\mu\text{m}$  gives a total luminosity of  $7.8 \times 10^{43}$  ergs  $\text{s}^{-1}$  which is comparable to that between 4000 Å and 2 keV ( $6.3 \times 10^{43}$  ergs  $\text{s}^{-1}$ ) assuming a power law with  $\alpha = 1.4$  as in section 4.1. This implies that any unseen ultraviolet component absorbed and then reradiated in the infrared can only be approximately double that inferred from direct observation and presents a problem for any model in which an unseen initially isotropic continuum of the strength deduced from the  $U$  parameter is reprocessed into the infrared. This argument may rule out normal dusty torus models for the cause of anisotropy in the case of NGC4151. However, models in which the infrared source is much smaller than the ENLR and in which the continuum was brighter in the past are still viable.

#### *Thick Accretion Disc.*

This idea is based on the model originally proposed by Lynden-Bell (1978) and discussed recently by Madau (1988) in which the walls of a thick accretion disc form a ‘funnel’ which directs the ultraviolet and X-ray radiation into oppositely pointed cones. In such a scenario, the emitted radiation encountering the walls of the funnel is reprocessed into further high energy radiation which can only escape at the poles. Given that the ultraviolet radiation in this model is in fact thermal and thus following the discussion of section 4.2 the anisotropy factor may be partially explained in this way, the anisotropy factor of order 10 that can be provided would be sufficient. In this case, no large infrared signal remains to be detected by IRAS. One problem with applying Madau’s model to NGC4151 is that it requires the luminosity to be close to the Eddington limit which would

imply a nuclear mass of order  $10^6$  solar masses in NGC4151. This would be in conflict with the higher values needed if the BLR motions are gravitational in origin (e.g. Clavel *et al.* 1987).

## 6. Conclusions

Our analysis of the ENLR lines tell us how bright the nucleus appears to the gas in that region. This is some 13 times brighter than a simple power law interpolation between ultraviolet and X-rays recently observed at Earth.

Explanations for this apparent discrepancy include an excess of photons over that power law associated, for example, with a thermal source and a delay-time explanation invoking a higher mean brightness of the nucleus over the last millenium. These do not explain the distribution of the ENLR on the sky which leads the majority of the authors of this paper to favour anisotropy. Anisotropy produced by absorption in a molecular torus is unlikely as there is no sign of the infrared reradiation expected on such a model. However, models in which the nuclear emission is anisotropic because of relativistic beaming or in which the absorber is a thick accretion disc reradiating anisotropically in the ultraviolet remain tenable.

If we viewed NGC4151 from our distance but with the same brightness as seen by the ENLR, we would see it as an object of magnitude  $\sim 9.7$  with an absolute magnitude  $M_V = -21.8 \pm 1.2$ .

In the case of anisotropy, our result calls into question the total luminosity that has usually been assumed for AGN. However because of the small opening angle of the cone, any anisotropy in NGC4151 is unlikely to have a major effect on the luminosity attributed to this galactic nucleus. The effects of anisotropy on the calculation of luminosities will be more striking in cases where we, unwittingly, view the object in the direction in which its brightness is boosted. This is particularly likely to be so for the objects of highest luminosity in any sample where selection will tend to make us compute too high a luminosity if we assume isotropy. Thus the highest quoted quasar luminosities may be overestimates of this type and may need downward revision by a factor of order 10 (but more if the anisotropy is greater) in these cases. Note, however, that, because the record AGN luminosity has increased since Lynden-Bell’s (1978) argument for a gravitational energy source for AGN was constructed, this remains valid today.

An anisotropy of a factor of order ten might have important effects for statistical studies; complete samples selected on the brightness of beamed emission components might have quite different properties from those selected using unbeamed ones.

*Acknowledgements.* The Lovers of Active Galaxies (LAG) collaboration was formed to seek the ‘‘International Time’’ on the Canarian telescopes offered by the *Comité Científico Internacional*. The authors together with J.Baruch, D.Carter, P.Coleman, S.Collin, M.Joly, C.Jenkins, J.Hough, A.López-Sainz, J.Lub, K.Mason, S.Nakatani and D.Péquinot comprise the collaboration. LAG is grateful for the generous allocation of time it received. The Isaac Newton Telescope, on the island of La Palma, is operated by the Royal Greenwich Observatory at the Spanish *Observatorio del Roque de los Muchachos* of the *Instituto de Astrofísica de Canarias*. The FIGARO software was provided by the UK SERC Starlink Project. PTO also acknowledges financial support from the SERC. MVP thanks the Institute of Astronomy, Cambridge for hospitality while this work was

done. AR would like to thank Luc Binette for providing the MAPPINGS program.

## References

- Aller, L.H.: 1987 *Physics of Thermal Gaseous Nebulae* D. Reidel Publishing Company, Dordrecht, The Netherlands.
- Antonucci, R.R.J. & Miller, J.S., 1985. *Astrophys. J.*, **297**, 621.
- Antonucci, R.R.J., 1988. Proceedings of *The 14th Texas Symposium on Relativistic Astrophysics*, New York Academy of Sciences, New York.
- Barthel, P., 1989. *Astrophys. J.*, **336**, 606.
- Bergeron, J., Boksenberg, A., Dennefeld, M. & Tarengi, M., 1983. *Mon. Not. R. astr. Soc.*, **202**, 125.
- Bergeron, J. & Durret, F., 1987. *Astr. astrophys.*, **184**, 93.
- Binette, L., Dopita, M.A. & Tuohy, I., 1985. *Astrophys. J.*, **297**, 476.
- Binette, L., Courvoisier, T. & Robinson, A.R., 1988. *Astr. astrophys.*, **190**, 29.
- Browne, I.W.A., 1989. Proceedings of ESO workshop on *Extranuclear Activity in Galaxies*, eds. Meurs, E. & Fosbury, R.A.E., Garching, May 16-18 1989.
- Bruhweiler, F.C. & Smith, A.M., 1988. *Astrophys. J.*, **327**, 664.
- Chelli, A., Perrier, C., Cruz-González, I. & Carrasco, L., 1987. *Astr. astrophys.*, **177**, 51.
- Clavel, J., Altamore, A., Perola, G.C., Boksenberg, A., Penston, M.V., Snijders, M.A.J., Bromage, G.E., Pelat, D., Elvius, A. & Ulrich, M.H., 1987. *Astrophys. J.*, **321**, 251.
- Cohen, R.D., 1983. *Astrophys. J.*, **273**, 489.
- Davies, R.D., 1973. *Mon. Not. R. astr. Soc.*, **161**, 25P.
- di Serego Alighieri, S., Binette, L., Courvoisier, T.J.-L., Fosbury, R.A.E. & Tadhunter, C.N., 1988. *Nature*, **334**, 591.
- Done, C., Ward, M.J., Fabian, A.C., Kuneida, H., Tsuruta, S., Lawrence, A., Smith, M.G. & Wamsteker, W., 1989. *Mon. Not. R. astr. Soc.*, (submitted).
- Edelson, R.A., Gear, W.K.P., Malkan, M.A. & Robson, E.I., 1988. *Nature*, **336**, 749.
- Elvis, M.S., Briel, U.G. & Henry, J.P., 1983. *Astrophys. J.*, **268**, 105.
- Fosbury, R.A.E., 1989. Proceedings of ESO workshop on *Extranuclear Activity in Galaxies*, eds. Meurs, E. & Fosbury, R.A.E., Garching, May 16-18 1989.
- Fuller, N.M.J., 1989. *Starlink User Note*, **86**, Rutherford and Appleton Laboratory.
- Harrison, B., Pedlar, A., Unger, S.W., Burgess, P., Graham, D.A. & Preuss, E., 1986. *Mon. Not. R. astr. Soc.*, **218**, 775.
- Heckman, T.M. & Balick, B., 1983. *Astrophys. J.*, **268**, 102.
- Johnstone, R.M. & Fabian, A.C., 1988. *Mon. Not. R. astr. Soc.*, **233**, 581.
- Kawara, K., Nishida, M. & Gregory, B., 1989. *Astrophys. J. Letts.*, **342**, L55.
- Khachikian, E.Y. & Weedman, D.W., 1974. *Astrophys. J.*, **192**, 581.
- Koski, A.T., 1978. *Astrophys. J.*, **223**, 56.
- Lynden-Bell, D., 1978. *Physica Scripta*, **17**, 185.
- Madau, P., 1988. *Astrophys. J.*, **327**, 116.
- Netzer, H., 1985. *Mon. Not. R. astr. Soc.*, **216**, 63.
- Netzer, H., 1987. *Mon. Not. R. astr. Soc.*, **225**, 55.
- Orr, M.J.L. & Browne, I.W.A., 1982. *Mon. Not. R. astr. Soc.*, **200**, 1067.
- Pedlar, A., Dyson, J.E. & Unger, S.W., 1985. *Mon. Not. R. astr. Soc.*, **214**, 463.
- Penston, M.V., Boksenberg, A., Bromage, G.E., Clavel, J., Elvius, A., Gondhalekar, P.M., Jordan, C., Lind, J., Lindegren, L., Perola, G.C., Pettini, M., Snijders, M.A.J., Tanzi, E.G., Tarengi, M. & Ulrich, M.H., 1981. *Mon. Not. R. astr. Soc.*, **196**, 857.
- Péquignot, D., 1986. *Workshop on Model Nebulae*, Publication de l'Observatoire de Paris, p.363.
- Pérez, E., González-Delgado, R.M., Tadhunter, C. & Tsvetanov, Z., 1989. *Mon. Not. R. astr. Soc.*, **241**, 31P.
- Pérez-Fournon, I. & Wilson, A.S., 1989. Proceedings of ESO workshop on *Extranuclear Activity in Galaxies*, eds. Meurs, E. & Fosbury, R.A.E., Garching, May 16-18 1989.
- Perola, G.C., Boksenberg, A., Bromage, G.E., Clavel, J., Elvius, M., Elvius, A., Gondhalekar, P.M., Lind, J., Lloyd, C., Penston, M.V., Pettini, M., Snijders, M.A.J., Tanzi, E., Tarengi, M., Ulrich, M.H. & Warwick, R.S., 1982. *Mon. Not. R. astr. Soc.*, **200**, 293.
- Pogge, R.W., 1988. *Astrophys. J.*, **328**, 519.
- Pogge, R.W., 1989. *Astr. J.*, **98**, 124.
- Robinson, A., Binette, L., Fosbury, R.A.E. & Tadhunter, C.N., 1987. *Mon. Not. R. astr. Soc.*, **227**, 97.
- Schmidt, G.D. & Miller, J.S., 1980. *Astrophys. J.*, **240**, 759.
- Schulz, H., 1988. *Astr. astrophys.*, **203**, 233.
- Stasińska, G., 1982. *Astr. astrophys. Suppl.*, **55**, 15.
- Tadhunter, C., 1989. *Proceedings of the XI European Regional Astronomy Meeting of the IAU, Tenerife*, in press.
- Tohline, J.E. & Osterbrock, D.E., 1982. *Astrophys. J. Letts.*, **252**, L49.
- Tsvetanov, Z., Tadhunter, C., Pérez, E. & González-Delgado, R., 1989. Proceedings of ESO workshop on *Extranuclear Activity in Galaxies*, eds. Meurs, E. & Fosbury, R.A.E., Garching, May 16-18 1989.
- Ulrich, M.-H., 1973. *Astrophys. J.*, **181**, 51.
- Unger, S.W., Pedlar, A., Axon, D.J., Whittle, M., Meurs, E.J.A. & Ward, M.J., 1987. *Mon. Not. R. astr. Soc.*, **228**, 671.
- Unger, S.W., Taylor, K., Pedlar, A., Ghataure, H., Penston, M.V. & Axon, D.J., 1989. *IAU Symposium*, **134**, Eds. D.E. Osterbrock & J.S. Miller; Kluwer Ac. Publ., p.331.
- Ward, M.J., 1988. *Nature*, **336**, 15.
- Ward, M.J., Done, C., Fabian, A.C., Tennant, A.F. & Schafer, R.A., 1988. *Astrophys. J.*, **324**, 767.
- Wilson, A.S. & Ulvestad, J.S., 1987. *Astrophys. J.*, **319**, 105.

This article was processed by the author using Springer-Verlag T<sub>E</sub>X AA macro package 1989.